Available online at www.sciencedirect.com

ScienceDirect

Mendeleev Commun., 2023, **33**, 269–271

Mendeleev Communications

Synthesis and photocatalytic activity of the Co-containing materials based on amorphous SiO_2

Ksenia I. Svetlakova,[a] Irina S. Mediankina,*[b] Liliya A. Pasechnik,[b] Larisa Yu. Buldakova[b] and Mikhail Yu. Yanchenko[b]

[a] *Institute of Chemical Engineering, Ural Federal University, 620002 Ekaterinburg, Russian Federation*
[b] *Institute of Solid State Chemistry, Ural Branch of the Russian Academy of Sciences, 620990 Ekaterinburg, Russian Federation. E-mail: lysira90@mail.ru*

DOI: 10.1016/j.mencom.2023.02.039

Functional materials based on highly dispersed amorphous silica and cobalt compounds have been obtained by solvothermal and mechanochemical methods. The formation of silicate $Co_3(Si_2O_5)_2(OH)_2$ under hydrothermal conditions has been established. This composition, in comparison with mechano-mixes, provides better photoactivity in the hydroquinone decomposition reaction under ultraviolet irradiation, herewith maintaining the surface characteristics of amorphous SiO_2.

Keywords: amorphous silica, cobalt silicate, hydrothermal synthesis, highly dispersed material, photocatalyst.

Mesoporous metal silicates and materials based on silicon oxide possess a high reactivity and ion exchange capacity due to the presence of surface functional groups and unique structural coordination of SiO_4 tetrahedra and metal–oxygen polyhedra. Such properties and low cost allow silicates to be widely used in sorption and catalytic processes for water purification, carbon monoxide conversion and cracking reaction.[1–3] Cobalt silicate is utilized in the ceramic industry as a heat- and light-resistant pigment. Its chromaticity and brightness are determined by the polarizability of cobalt ions.[4] The necessary features for creating anode layers of lithium-ion batteries,[5] capacitors, electromagnetic emission absorbers and magnetic materials with Co_2SiO_4 are high stability and activity. These properties are achieved using expensive organosilicon compounds in synthesis and high-temperature annealing (above 1300 °C).[6,7] Currently, there is a great concern about environmental problems, the removal of organic pollutants from wastewater being among the urgent tasks. Specific surface area of a catalyst is the most important parameter defining the activity of the catalyst in degradation reactions of pesticides, dyes, and industrial chemicals in aqueous media.[8] Due to the combination of high activity, chemical stability, nontoxicity and availability titanium dioxide is one of the most commonly used photocatalytic materials.[9] However, it also has a number of disadvantages, *i.e.*, limited absorption spectrum and fast charge carrier recombination. Not the least valuable and promising is highly dispersed silica possessing a small particle size, developed surface, and hydrophobic properties. The introduction of cobalt ions was reported to expand the operating spectral band and impart additional functional characteristics.[4] Creating the materials that combine unique surface characteristics and high reactivity is an upcoming trend in the development of photocatalysis.

The main role in the formation of materials with desired photocatalytic properties (*e.g.*, morphology and surface area) belongs to the synthesis method.[10] Silica similar to white soot was obtained earlier from a fluorosilicate solution during processing of silicon-containing technogenic waste.[11] Addition of the active component under soft solvothermal conditions makes it possible to form the required final composition of the product and to control the particle morphology.[12] No less attractive and environmentally friendly process eliminating the formation of effluent stream is the mechanochemical method of synthesis and modification of oxide materials properties.[13] In this work, we obtained cobalt-containing materials based on amorphous silica by two abovementioned methods for comparative characterization of the composition, structural and photocatalytic properties.[†]

[†] The initial reagents of analytical grade were ammonium biflouride (NH_4HF_2), cobalt formate [$Co(COOH)_2 \cdot 2H_2O$], cobalt oxalate ($CoC_2O_4 \cdot 2H_2O$), ammonia ($NH_3 \cdot H_2O$) and ammonium chloride (NH_4Cl). The cobalt oxide Co_3O_4 was obtained by calcination of $CoC_2O_4 \cdot 2H_2O$ at 300 °C for 4 h. Amorphous silicon oxide (SiO_2) was precipitated by $NH_3 \cdot H_2O$ from $(NH_4)_2SiF_6$ solution and dried at 120 °C.[11] In hydrothermal synthesis, SiO_2 (0.5 g) was dispersed in distilled water (50 ml) using an ultrasonic bath for 40 min, then $NH_3 \cdot H_2O$ solution (1 ml), NH_4Cl (0.5 g) and 1.70 or 170 ml of 9.0 g dm^{-3} $Co(COOH)_2$ solution for the samples S3 or S4, respectively, were added. The reaction mixture after holding in an autoclave at 100 °C for 10 h was separated by centrifugation at 3000 rpm. The precipitate was washed with water up to pH 5–6, then with ethanol and dried at 120 °C. In the mechanochemical method, oxides in given ratios were intensively ground for 2 h in a ceramic mortar in the presence of ethanol and then dried at 120 °C.

X-ray powder diffraction (XRD-7000 diffractometer, Shimadzu) using CuKα radiation in the 2θ range 5–70° with a step of 0.03° was employed. The morphological peculiarities were examined by the scanning electron microscopy (SEM) on a JEOL JSM 6390 LA microscope. The stoichiometry of the elements was confirmed by energy dispersive X-ray (EDX) analysis with an EX-23010BU analyzer. The specific surface area and porosity were determined using the BET model with a Gemini VII 2390 surface area analyzer TriStar 3000 (Micromeritics). The pycnometric density was measured by a helium pycnometer with a cell volume of 1 cm^3 (AccuPyc II 1340). Silicon powder was used as a standard.

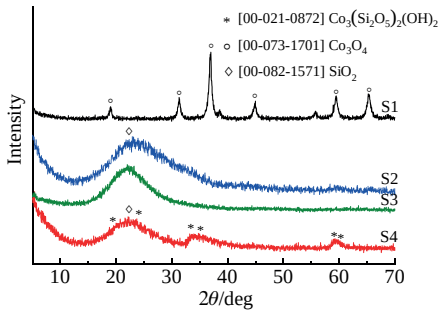

Figure 1 XRD patterns of oxides (S1) Co_3O_4 and (S2) SiO_2 and samples S3 and S4.

The XRD patterns of initial silicon and cobalt oxides as well as the products of hydrothermal synthesis are shown in Figure 1. As can be seen, the main phase in samples S3 and S4 (Table 1) is amorphous SiO_2 that appears as a halo in the 2θ angular region of 20–30°. Reduction of the halo and appearance of two new peaks for the sample S4 are related to the hydroxysilicate phase of the composition $Co_3(Si_2O_5)_2(OH)_2$ possessing a weak crystallinity. Thus, hydrothermal treatment at 100 °C caused interaction of silica with cobalt ions in the solution that resulted in the formation of a new compound. At a significantly lower amount of cobalt ions in the initial reaction mixture, no new phases were found in S3. The X-ray patterns of mechanosynthesis products S5 and S6 represent a total set of reflections of the initial oxides.

The IR spectra (Figure 2) of Si-containing samples revealed predominance of the absorption bands at 1090 cm^{-1} related to the stretching vibrations Si–O–Si bonds of silica as a base. At the same time, all spectra exhibit broad bands in the range of 3200–3500 cm^{-1} up to 3750 cm^{-1}, attributed to the stretching vibrations, and weak peak at 1600 cm^{-1} corresponding to the deformation vibrations of H–O–H bonds of adsorbed and structural water.[15] For mechanosynthesis products S5 and S6 the total effect of the spectra is also observed, which is most clearly manifested at a ratio of Co : Si = 1 : 1 in the sample S6 with an increase in the number of Si–O and Co–O bonds bands in the range from 1000 to 500 cm^{-1}. The peak intensity decreases at 800 cm^{-1}, red shift and stronger splitting of the stretching vibration band of Si–O–Si at 1035 cm^{-1} confirm distortion and coordination of SiO_4^- tetrahedron with cobalt ions forming Co–O–Si bonds in cobalt silicate (Figure 2, curve of sample S4). If the formation of crystalline metal silicates with a stable structure occurs, the stretching vibrations in the range of 650–800 cm^{-1} would appear as stronger narrow bands with possible splitting.

Table 1 Composition, method of synthesis and surface characteristics of samples.

Sample	Composition	Method of synthesis	Specific surface area/ $m^2\ g^{-1}$	Micropore area/ $m^2\ g^{-1}$	Micropore volume/ $cm^3\ g^{-1}$
S1	Co_3O_4	–	65.19	–	–
S2	SiO_2	–	234.52	0.02	49.74
S3	Co : Si (1 : 100)	hydrothermal	135.59	9.31	⩽0.01
S4	Co : Si (1 : 1)	hydrothermal	79.91	1.61	⩽0.01
S5	Co : Si (1 : 100)	mechanochemical	161.01	1.59	0.99
S6	Co : Si (1 : 1)	mechanochemical	115.96	2.19	0.88

IR spectra were recorded on a Nicolet 6700 Thermo Scientific spectrometer over 400–4000 cm^{-1}. The photocatalytic activity of the products was evaluated by oxidation of benzene-1,4-diol under UV irradiation. The solutions were irradiated in quartz cuvettes using a BUV-15 lamp (λ_{max} = 253 nm). The concentration of hydroquinone was monitored by the voltametric method using a PU-1 polarography.[14]

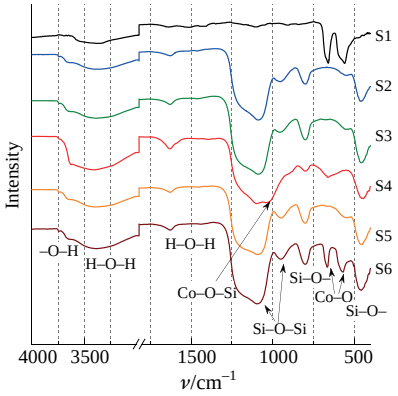

Figure 2 IR spectra of oxides S1 (Co_3O_4), S2 (SiO_2), and samples S3–S6.

The SEM studies confirm the assumption that the highly dispersed amorphous silica particles of sample S2 retain their shape in the products S3–S6 as shown for the sample S4 (Figure 3). According to Figure 3(*a*),(*c*), all silica containing samples possess the grain structure of less than 1 μm in size agglomerated into clusters of micrometer size. For the initial Co_3O_4 the persistence of the acicular-lamellar shape of the starting cobalt acetate particles with a wide size distribution is observed, which is easily and completely destroyed by grinding. The distribution of X-ray contrast of the images in the backscatter electron mode is homogeneous. EDC elemental mapping for all hydrothermal products indicates the absence of a second phase with a predominant content of each element in the form of individual inclusions.

The surface properties and dispersion of materials were characterized by the specific surface area, micropore area and volume (see Table 1) that are crucial for adsorption and catalysis in terms of capacity and efficiency. The developed surface provides a sufficient number of active centers, thereby increasing the solid–liquid contact area and reducing the mass transfer length in the solid phase. According to the results of BET analysis, a substantional decrease in the specific surface area in comparison with initial silica in S2 has been observed for all products. The data in Table 1 show that any impact essentially changes the porous structure of the original amorphous silica. The strongest decrease in the specific surface area and pore volume has been revealed in the case of formation of $Co_3(Si_2O_5)_2(OH)_2$ in S3, which possesses the largest micropore area among other compounds.

The results of photocatalytic study on the example of hydroquinone decomposition upon UV irradiation (253 nm) are shown in Figure 4. Hydroquinone was chosen due to its light stability compared with other dyes such as methylene blue. The materials tested exhibited better hydroquinone degradation properties in comparison with a blank run (reaction without catalyst). Pure cobalt oxide S1 was the most aggressive towards hydroquinone owing to its high chemical activity. Despite the fact that the specific surface area of cobalt hydroxysilicate particles is two times less than that of the original silica, the use of S3 sample resulted in the decomposition of about 90% of the organic substance in 12 h. An increase in the amount of cobalt in S4 did not result in activity enhancement because of the worse surface characteristics of the sample.

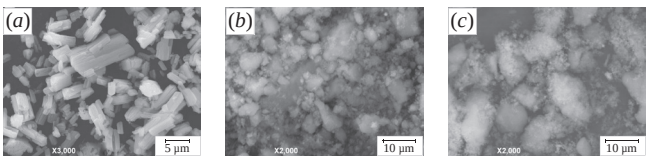

Figure 3 SEM images of samples (*a*) S1, (*b*) S2 and (*c*) S4.

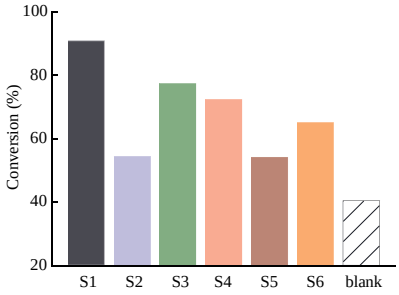

Figure 4 Conversion degree of hydroquinone upon UV irradiation for 12 h in the presence of samples S1–S6.

However, the fact that similar results were obtained over the entire duration of catalysis using the products of hydrothermal synthesis S3 and S4 indicates a high activity of even a small number of active centers formed on a highly developed surface, in particular, for Co–O–Si bonds. The behavior of mechanosynthesis products S5 and S6 with respect to hydroquinone correlates with the composition rather than with the specific surface area. The S5 sample consisting almost exclusively of silica and having, at the same time, a highly developed surface demonstrated the result comparable to silica. To explore the mechanism of photocatalytic action of the resulting phase $Co_3(Si_2O_5)_2(OH)_2$ as part of the material based on highly dispersed amorphous silica is the purpose of the further work .

In summary, the use of silica and cobalt formate as initial reagents enables formation of hydroxosilicate $Co_3(Si_2O_5)_2(OH)_2$ under low-temperature hydrothermal conditions. Reduction of the amount of cobalt ions in the initial mixture contributes to a higher degree of hydroquinone decomposition (about 80%) during UV irradiation for 12 h owing to the developed surface of silica matrix and high reactivity of the produced $Co_3(Si_2O_5)_2(OH)_2$. The catalytic properties of mechanical oxide mixtures are largely determined by the cobalt content, the surface characteristics achieved by dispersion being similar. Our results suggest that the hydrothermal method holds promise for creation of photocatalytically active materials based on amorphous silica.

The work was carried out within the framework of the state task of the Institute of Solid State Chemistry of the Ural Branch of the Russian Academy of Sciences (subject no. AAAA-A19-119031890028-0).

References

1 J. Qu, W. Lee, C.-Y. Cao, X.-J. Yin, L. Zhao, J. Bai, Z. Qin and W.-G. Song, *J. Mater. Chem*., 2012, **22**, 17222.
2 S.-M. Hao, M.-Y. Yu, Y.-J. Zhang, Y. Abdelkrim and J. Qu, *J. Colloid Interface Sci*., 2019, **545**, 128.
3 L. V. Sineva, E. O. Gorokhova, E. A. Pushina, E. V. Kulchakovskaya and V. Z. Mordkovich, *Mendeleev Commun.*, 2020, **30**, 362.
4 I. V. Pishch, G. N. Maslennikova, K. B. Podbolotov, Yu. A. Karizna and I. V. Belyakovich, *Glass Ceram*., 2011, **68**, 71 [*Steklo i Keramika*, 2011, **84** (3), 3].
5 D. Lan, Z. Gao, Z. Zhao, G. Wu, K. Kou and H. Wu, *Chem. Eng. J*., 2021, **408**, 127313.
6 J. Yatabe, T. Sugizaki, T. Ikawa and T. Kageyama, *J. Ceram. Soc. Jpn*., 1979, **105**, 188.
7 D. A. Khanin, Yu. N. Kononevich, V. P. Morgalyuk, M. N. Temnikov, V. G. Vasil'ev, V. K. Brel and A. M. Muzafarov, *Mendeleev Commun.*, 2022, **32**, 234.
8 H. Jeong, T. Kim, D. Kim and K. Kim, *Int. J. Hydrogen Energy*, 2006, **31**, 1142.
9 D.-H. Lee, K.-S. Park, C.-G. Lee and B. Swain, *J. Photochem. Photobiol., A*, 2020, **400**, 112654.
10 O. I. Gyrdasova, E. V. Shalaeva, V. N. Krasil'nikov, L. Yu. Buldakova, I. V. Baklanova, M. A. Melkozerova, M. V. Kuznetsov and M. Yu. Yanchenko, *Mater. Charact*., 2021, **179**, 111384.
11 I. S. Medyankina and L. A. Pasechnik, *AIP Conf. Proc*., 2020, **2313**, 050020.
12 T. P. Maslennikova and E. N. Gatina, *Russ. J. Appl. Chem*., 2018, **91**, 286 (*Zh. Prikl. Khim*., 2018, **91**, 238).
13 O. V. Lapshin, E. V. Boldyreva and V. V. Boldyrev, *Russ. J. Inorg. Chem*., 2021, **66**, 433 (*Zh. Neorg. Khim.*, 2021, **66**, 402).
14 O. I. Gyrdasova, N. S. Sycheva, I. V. Baklanova, L. Yu. Buldakova, M. Yu. Yanchenko, K. V. Nefedova and V. N. Krasil'nikov, *J. Mater. Sci.: Mater. Electron*., 2019, **30**, 8820.
15 L. M. Kustov and A. L. Kustov, *Mendeleev Commun*., 2021, **31**, 526.

Received: 2nd August 2022; Com. 22/6975